



**HAL**  
open science

## The very large electrode array for retinal stimulation (VLARS)-A concept study

Tibor Karl Lohmann, Florent Haiss, Kim Schaffrath, Anne-Christine Schnitzler, Florian Waschkowski, Claudia Barz, Anna-Marina van Der Meer, Claudia Werner, Sandra Johnen, Thomas Laube, et al.

### ► To cite this version:

Tibor Karl Lohmann, Florent Haiss, Kim Schaffrath, Anne-Christine Schnitzler, Florian Waschkowski, et al.. The very large electrode array for retinal stimulation (VLARS)-A concept study. *Journal of Neural Engineering*, 2019, 16 (6), pp.066031. 10.1088/1741-2552/ab4113 . pasteur-03291827

**HAL Id: pasteur-03291827**

**<https://pasteur.hal.science/pasteur-03291827>**

Submitted on 19 Jul 2021

**HAL** is a multi-disciplinary open access archive for the deposit and dissemination of scientific research documents, whether they are published or not. The documents may come from teaching and research institutions in France or abroad, or from public or private research centers.

L'archive ouverte pluridisciplinaire **HAL**, est destinée au dépôt et à la diffusion de documents scientifiques de niveau recherche, publiés ou non, émanant des établissements d'enseignement et de recherche français ou étrangers, des laboratoires publics ou privés.



Distributed under a Creative Commons Attribution 4.0 International License

# The very large electrode array for retinal stimulation (VLARS)—A concept study

Tibor Karl Lohmann<sup>1,7</sup> , Florent Haiss<sup>4,5</sup> , Kim Schaffrath<sup>1</sup>,  
Anne-Christine Schnitzler<sup>1</sup>, Florian Waschowski<sup>2</sup> , Claudia Barz<sup>1,3,4</sup>,  
Anna-Marina van der Meer<sup>1</sup>, Claudia Werner<sup>1</sup>, Sandra Johnen<sup>1</sup>,  
Thomas Laube<sup>6</sup>, Norbert Bornfeld<sup>4</sup>, Babak Ebrahim Mazinani<sup>1</sup>,  
Gernot Rößler<sup>1</sup>, Wilfried Mokwa<sup>2</sup> and Peter Walter<sup>1</sup>

<sup>1</sup> Department of Ophthalmology, University Hospital RWTH Aachen, Aachen, Germany

<sup>2</sup> Institute for Materials in Electric Engineering I, RWTH Aachen University, Aachen, Germany

<sup>3</sup> Institute of Neuroscience and Medicine, INM-10, Research Centre Jülich, Jülich, Germany

<sup>4</sup> Interdisciplinary Center of Clinical Research IZKF, Neuroscience Group, RWTH Aachen University, Aachen, Germany

<sup>5</sup> Unit of Neural Circuit Dynamics and Decision Making, Institut Pasteur, Paris, France

<sup>6</sup> Department of Ophthalmology, University Hospital Essen, Essen, Germany

E-mail: [tlohmann@ukaachen.de](mailto:tlohmann@ukaachen.de)

Received 3 April 2019, revised 7 August 2019

Accepted for publication 3 September 2019

Published 6 November 2019



## Abstract

**Objective.** The restoration of vision in blind patients suffering from degenerative retinal diseases like retinitis pigmentosa may be obtained by local electrical stimulation with retinal implants. In this study, a very large electrode array for retinal stimulation (VLARS) was introduced and tested regarding its safety in implantation and biocompatibility. Further, the array's stimulation capabilities were tested in an acute setting. **Approach.** The polyimide-based implants have a diameter of 12 mm, cover approximately 110 mm<sup>2</sup> of the retinal surface and carrying 250 iridium oxide coated gold electrodes. The implantation surgery was established in cadaveric porcine eyes. To analyze biocompatibility, ten rabbits were implanted with the VLARS device, and observed for 12 weeks using slit lamp examination, fundus photography, optical coherence tomography (OCT) as well as ultrasound imaging. After enucleation, histological examinations were performed. In acute stimulation experiments, electrodes recorded cortical field potentials upon retinal stimulation in the visual cortex in rabbits. **Main results.** Implantation studies in rabbits showed that the implantation surgery is safe but difficult. Retinal detachment induced by retinal tears was observed in five animals in varying severity. In five cases, corneal edema reduced the quality of the follow-up examinations. Findings in OCT-imaging and funduscopy suggested that peripheral fixation was insufficient in various animals. Results of the acute stimulation demonstrated the array's ability to elicit cortical responses. **Significance.** Overall, it was possible to implant very large epiretinal arrays. On retinal stimulation with the VLARS responses in the visual cortex were recorded. The VLARS device offers the opportunity to restore a much larger field of visual perception when compared to current available retinal implants.

<sup>7</sup> Author to whom any correspondence should be addressed.



Original content from this work may be used under the terms of the [Creative Commons Attribution 3.0 licence](https://creativecommons.org/licenses/by/3.0/). Any further distribution of this work must maintain attribution to the author(s) and the title of the work, journal citation and DOI.

Keywords: retinal stimulation, retina implant, multielectrode array, cortical activation, local field potentials, biocompatibility, vitreoretinal surgery

(Some figures may appear in colour only in the online journal)

## 1. Introduction

Retinitis pigmentosa (RP) is a retinal dystrophy leading to blindness due to several mutations in genes encoding for key proteins involved in the basic visual processes [1]. The disease remains a leading cause of blindness in developed countries [2]. To this day, no adequate therapy is available for the very advanced stages of complete or near complete blindness. Through the course of the disease, photoreceptor cell degeneration leads to progressive visual impairment, although neural cells of the inner retina remain functional [3, 4]. Thus, targeting these cellular structures using retinal implant systems for electrical stimulation can restore meaningful visual perception in patients [5–7].

Targeting the retina has shown benefits in terms of surgical feasibility and a relatively low risk profile compared to stimulation of the cortex or the optic nerve [8, 9]. Also, the inherent retinotopy and neuronal modulation of elicited phosphenes can be used to further improve the visual perception of subjects implanted with retinal stimulator systems.

The epiretinal *Argus II* and the subretinal *Alpha IMS resp. AMS* systems are approved for clinical use in the EU and the US. Currently approximately 350 patients received an *Argus II* (Second Sight, Sylmar, CA, USA) implant and approximately 100 received the *Alpha IMS resp. AMS* implant (Retina Implant AG, Reutlingen, Germany) [10, 11]. However, using these prostheses, visual rehabilitation is limited. Patients with RP are suffering from a progressive narrowing of the visual field [12]. The currently available systems only restore a visual field of approximately 10° visual angle requiring scanning of the area either with eye or head movements [13]. Studies assume that a visual field of about 27° and 256 electrodes are needed to obtain a visual field sufficiently granting orientation and movement, which exceeds the capability of the currently available systems [13]. Thus, to restore a wider visual field, larger implants are necessary. We developed a flexible and thin retinal implant consisting of a multielectrode array approximately three times the size of the comparable epiretinal *Argus II* device and mounting 250 electrodes for epiretinal stimulation, which we called the very large array retinal stimulator (VLARS) [14].

The conducted concept study was focused on the surgical feasibility and biocompatibility of the VLARS structures, as well as preliminary testing its efficacy.

Firstly, cadaveric porcine eyes were used to establish an implantation procedure. Secondly, implantations in rabbits were conducted. During a 12-week follow-up, the biocompatibility of the large multielectrode array implants was examined. Thirdly, acute stimulation experiments were performed to evaluate cortical responses induced by electrical stimulation of the retina.

## 2. Materials and methods

### 2.1. Fabrication of the device and device parameters

Design, fabrication and electrochemical functionality testings of the VLARS were previously published [14].

In brief, the VLARS multielectrode arrays (MEA) were designed using the simulation software COMSOL (COMSOL AB, Stockholm, Sweden). A base layer of polyimide was spin coated on a metalized silicon wafer and polymerized at 400 °C. The gold leads and stimulating electrodes were electroplated on the polyimide layer with a thickness of 2.5 μm and covered with another layer of polyimide. The entire structure was encapsulated with the hydrophobic and biocompatible polyimide *Parylene C* for isolation and durability. The gold electrodes were coated with platinum and reactively sputtered with iridium oxide for low electrode impedance resulting in lower voltages during stimulation. Figure 1 shows four schematic designs from an early stage of development: a circular, a spiral, a star, and a globe shaped array.

Subsequent altering of the thickness of the *Parylene C* layer on one side of the array and introducing the array to thermal contact treatment of 125 °C–155 °C for five minutes resulted in an inherent curvature of the devices. Depending on the annealing temperature, the time of temperature exposition, the thickness of the *Parylene C* coating and the parameters of the deposition process, the contraction, thus the inherent curvature can be modified [15]. Two arrays were curved following this technique prior to implantation in rabbit eyes.

During the implantation in cadaveric porcine eyes the star and the globe shaped structures were tested. During the biocompatibility study in rabbit eyes, solely the star shaped array was implanted. Both designs have a central aperture and apertures on the peripheral edges (figure 6(B), star shaped array) suitable for epiretinal fixation with retinal tacks (Geuder AG, Heidelberg, Germany).

The arrays measure 12 mm in diameter and cover approximately 110 mm<sup>2</sup> resulting in a visual angle of 37.6° or a visual field of 18.8°, respectively. Both designs mount 250 individual electrodes, each having a diameter of 100 μm except the larger return electrode at the base of the array's connecting lead that has a diameter of 1 mm. The electrodes' density is higher towards the array's center with a pitch of 300 μm, thus mimicking the distribution of photoreceptor and postsynaptic cells in the retina (figure 6(B)).

### 2.2. Device handling: implantation in cadaveric porcine eyes

To establish a safe and feasible surgery process, the implantation was initially tested in cadaveric porcine eyes, that were obtained from a local abattoir. For the implantation surgery,

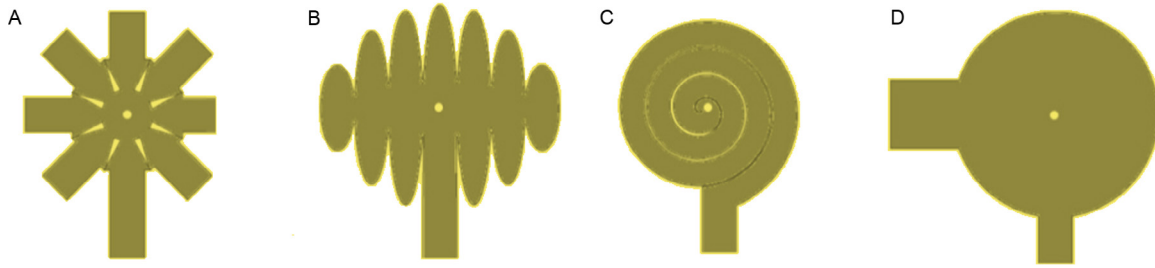


**Figure 1.** Schematic design of the VLARS early in development. (A) Early star shaped design. (B) Early globe shaped design. (C) Spiral shaped design. (D) Circular shaped design.

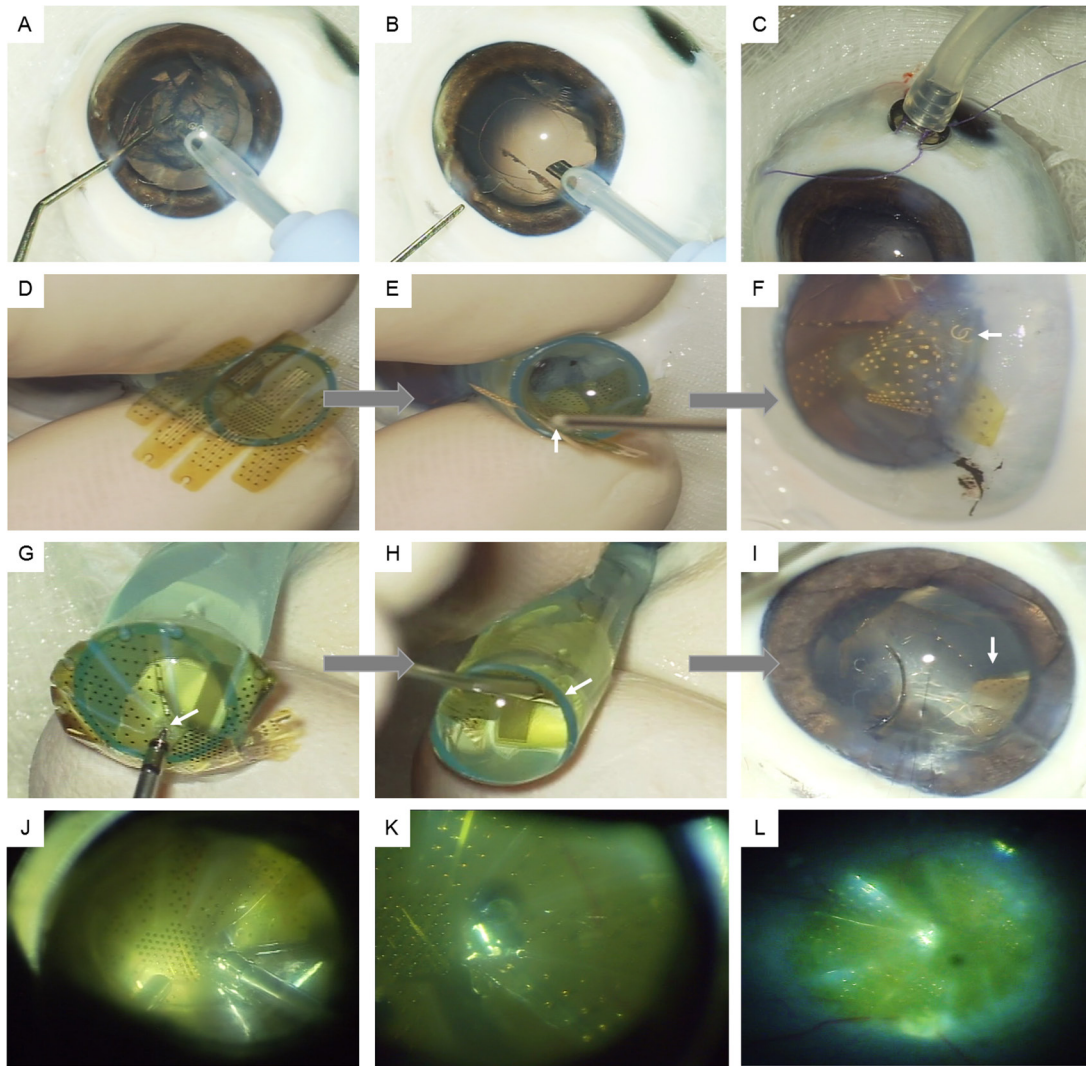


**Figure 2.** Implantation procedure of the VLARS in a cadaveric porcine eye. Note that (D)–(F) show the implantation of the globe shaped array in comparison to the implantation of the star shaped array shown in (G) to (L). (A) and (B) Phacoemulsification of the lens; (C) Fixation of the 20 Ga infusion; (D) to (F): Insertion of the globe shaped VLARS using the implantation cone. (D) The globe shaped array on top of the implantation cone. (E) Pushing the array forward with the retinal tack holder (arrow). (F) Poor positioning of the array in the anterior chamber (arrow shows overlapping peripheral apertures). (G)–(I) Insertion of the star shaped VLARS using the implantation cone. (G) The star shaped array on top of the implantation cone. The retinal tack is pushed through the aperture to move the array through the cone (arrow). (H) Pushing the array forward with the retinal tack holder (arrow). Note the concentric folding of the VLARS. (I) Good positioning of the array in the anterior chamber. A wing of the star shaped array is clearly observable on the right side (arrow). (J) Inserting the retinal tack; (K) Retinal tack in central aperture fixating the VLARS on the retinal pole (as seen through a 60D Kilp’s lens), (L) VLARS in position on the posterior retinal pole.

the eyes were fixated on an implantation socket. The surgery was performed using a surgical microscope (Zeiss Model OPMI 6-CFR XY, S5 Tripod, Carl Zeiss AG, Jena, Germany).

Lensectomy was performed via a 2.5 mm corneal incision using a standard phacoemulsification technique (OMNI, Fritz Ruck Ophthalmologische Systeme, Eschweiler, Germany)

(figures 2(A) and (B)). For pars plana vitrectomy, three 20 G scleral incisions were placed for the infusion, the light source and vitreous surgery instruments (Fritz Ruck Ophthalmologische Systeme, Eschweiler, Germany). For infusion (figure 2(C)), buffered saline solution (BSS, Alcon, Fort Worth, USA) was used. The posterior capsulorhexis was performed with the 20 G cutter to eventually protrude the VLARS structure from the anterior chamber towards the posterior pole of the retina after completing the vitrectomy. To support retinal attachment and safely lower the VLARS on the posterior pole, perfluorocarbon liquid (PFCL) (F-Decalin 1.93 g cm<sup>-3</sup> Fluoron GmbH, Ulm, Germany) was injected into the eye. The VLARS was pushed into the anterior chamber using the implantation cone positioned in the enlarged corneal opening (enlarged to approx. 5 to 6 mm) (figure 2(E)). The implantation cone was a modified pipette tip (Eppendorf AG, Hamburg, Germany). To reduce adhesion of the array to the cone's inner surface it was filled with a cohesive viscoelastic fluid (*Healon*, Johnsen and Johnson, New Brunswick, USA). The corneal incision was sutured with *Nylon 10-0* threads (Alcon, Fort Worth, USA). Once inside the eye, the array was unfolded, displaced from the anterior chamber towards the vitreous cavity and sunk on the PFCL bubble placed covering the posterior pole (figure 2(F)). Removing of the PFCL with a 32 G cannula led to the positioning of the VLARS. The VLARS was fixated on the posterior retinal pole by inserting a titanium retinal tack (Fa. Geuder, Heidelberg, Germany) through the array's central aperture (figure 2(J)). Once the intraocular manipulators and the infusion were removed, the pars-plana incisions were sutured with *Vicryl 7-0* threads (Alcon, Fort Worth, USA). The final position of the retinal tack and the VLARS was reassured using a 60 D lens (Kilp lens 60D, 20°, Geuder AG, Heidelberg, Germany) (figure 2(K)).

### 2.3. Implantation in rabbit eyes

All animal experiments, both in the semi-chronic implantation and the acute stimulation experiments, were performed according to the ARVO declaration for the use of animals in research and adhered to the 'Principles of laboratory animal care' (NIH publication No. 85-23, revised 1985), the OPRR Public Health Service Policy on the Human Care and Use of Laboratory Animals (revised 1986) and the U.S. Animal Welfare Act, as well as according to the German Law for the Protection of Animals and after obtaining approval by local authorities and ethics committee.

Inactive arrays were used to test the surgical implantation and biocompatibility *in vivo*. The stimulators were implanted into the right eye of ten rabbits (four *Chinchilla Bastard*, six *New Zealand White*). The animals were housed under standard conditions with an even 12-hour light/dark cycle and had access to food and water *ad libitum*. Implantation was performed following the protocol established during the implantation experiments in cadaveric porcine eyes, as described above.

Prior to the surgery, the rabbits received topical anesthesia by applying *proxymetacaine hydrochloride 0.5%* eye drops (Proparacain-POS, Ursapharm, Saarbrücken, Germany), as well as dilating eye drops containing *phenylephrine*

*hydrochloride 2.5%* and *tropicamide 0.5%* (MS-mydratic eye drops, Pharmacy of the RWTH Aachen University, Germany).

During the surgery in *Chinchilla Bastard* rabbits, 4–5 mg per kg bodyweight *xylazine* (Xylazin 2% Bernburg®, Medistar, Ascheberg, Germany) and 50 to 70 mg per kg bodyweight *ketamine* (Ketamin 10%, Ceva Tiergesundheit GmbH, Düsseldorf, Germany) were used as anesthetics. For the *New Zealand White* rabbits, 0.1 mg per kg bodyweight *xylazine* and 20 mg per kg bodyweight *ketamine* were used. The surgical field was treated with 10% *povidone-iodine* solution (Betaisodonna, Mundipharma GmbH, Limburg, Germany) for disinfection.

To adjust the eye position during surgery, incisions in the conjunctiva were performed, two opposing straight ocular muscles were hooked and looped with *Ethilon 5-0* threads (Alcon, Fort Worth, USA). The sclerotomies were done in 1.5 mm distance to the limbus. During 20 G vitrectomy, *triamcinoloneacetonide* 10 mg ml<sup>-1</sup> (Volon A 10 mg-Kristallsuspension, Dermapharm AG, Grünwald, Germany) was injected to facilitate vitreous removal. The array was advanced into the anterior chamber via the implantation cone shown above, as well as advanced directly through the corneal incision using various surgical devices: a tear duct probe, a push-pull manipulator, as well as several types of surgical forceps (Geuder AG, Heidelberg, Germany). After placing the VLARS on top of the PFCL bubble on the posterior retinal pole, the array was fixated using a titanium retinal tack (Fa. Geuder, Heidelberg, Germany), as described above. To complete the surgery the eye was filled with air.

At the end of the surgery, the animals received an intracameral injection of 750 mg *cefuroxime* (Cefuroxim Fresenius 750 mg, Fresenius Kabi DE, Bad Homburg, Germany) and 4 mg *dexamethasondihydrogenphosphat-Dinatrium* (Fortecortin Inject 4 mg, Merck KGaA, Darmstadt, Germany), as well as subconjunctival injection of *gentamicin* 8 mg (Gentamicin 8 mg Rotexmedica, ROTEXMEDICA GmbH Arzneimittelwerk) and 50 mg *prednisolon-21-succinat* (Prednisolon H 50 mg, Merck KGaA, Darmstadt, Germany) to prevent infection and reduce inflammation.

Clinical examinations evaluating appearance and behaviour of the animals were conducted daily. 20 mg of the non-steroidal anti-inflammatory drug *carprofen* (Rimadyl 20 mg, Zoetis GmbH, Berlin, Germany) was given once a day for three days after the surgery. Antibiotic and anti-inflammatory ointment and eyedrops (Isopto-Max Augensalbe, Dexamethason 1 mg g<sup>-1</sup>, Neomycin 3500 IE g<sup>-1</sup>, Polymyxin-B-sulfat 6000 IE g<sup>-1</sup>, Novartis Pharma, Basel, Switzerland) as well as mydratic eyedrops (MS-mydratic eye drops, Pharmacy of the RWTH Aachen University, Germany) to prevent synechia were applied twice daily for at least seven days, and in some cases longer depending on presence of inflammation.

### 2.4. Follow-up in the semi-chronic implantations

The follow-up was conducted for 12 weeks, using slit lamp examination, funduscopy, ultrasound imaging, spectral domain optical coherence tomography (SD-OCT) and fundus photography. They were conducted in general anaesthesia

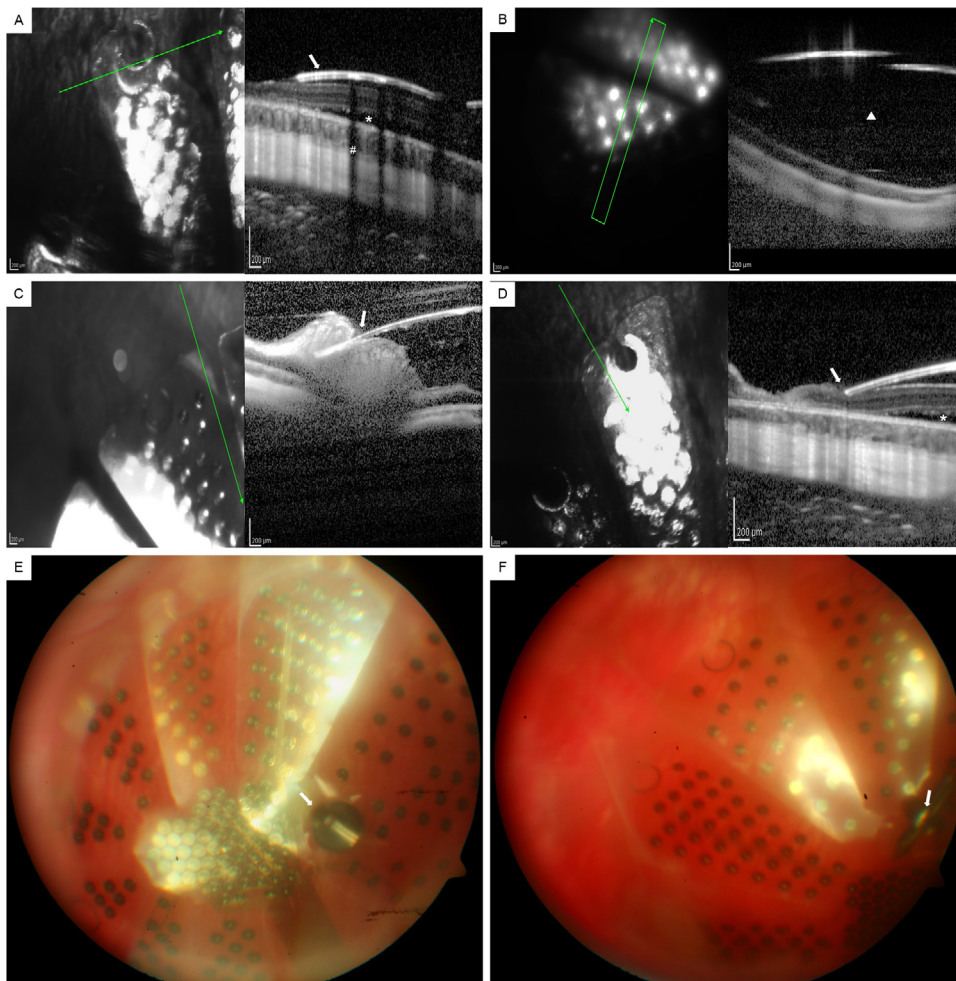


**Figure 3.** OCT-imaging and fundus photography of the VLARS after implantation. (A)–(D) *En-face* infrared (left side) and OCT-imaging (right side) of the implanted VLARS. The arrow in the infrared image on the left-hand side indicates the position and direction of the OCT-image. (A) (Animal 2): close alignment of the peripheral segment of the array (arrow) to the retinal surface (one week after implantation). Note subretinal fluid (asterix) and the artifact casted by the gold edging of the peripheral aperture (diamond sign). (B) (Animal 1): gap between the retinal surface and the peripheral segment of the array (triangle) (7 weeks after implantation). (C) (Animal 1): protrusion of the array into the retina (arrow) (12 weeks after implantation). (D) (Animal 2): the array's edge puts pressure on the retinal surface (arrow) (one week after implantation). Note subretinal fluid (asterix). (E) and (F) Fundus photography 12 weeks after implanting the VLARS. (E) (Animal 2) and (F) (Animal 5): the VLARS on the retinal pole. Note the difference in reflection of the VLARS' surface hinting an elevation of the wings. The retinal tack is highlighted with an arrow.

using *ketamine* and *xylazine* as described above. The animals underwent these follow-up diagnostics 1, 2, 4, 6, 8 and 12 weeks after implantation.

**2.4.1. Slit lamp examination and funduscopy.** For a clinical evaluation of the anterior segment a manual slit lamp was used (Bonnoskop II Mod. 66, hand piece: Carl Zeiss AG, Jena, Germany). Funduscopy was achieved using a 20D lens (Volk Optical Inc., Mentor, USA). Main points of interest were signs of inflammation or infection around the implanted eye, corneal clarity, signs of inflammation in the anterior chamber, presence of hyphema as well as vitreal blood, fundus visibility, position and fixation of the VLARS.

**2.4.2. Fundus photography.** For fundus photography, a *Zeiss FF450Plus* camera system (Carl Zeiss AG, Jena, Germany) with a *Canon EOS 5D* digital camera capturing system (Canon Inc., Tokyo, Japan) was used. In cases of good visibility, the

array's position was determined by the fixation of the retinal tack and the displacement of the array's wings.

**2.4.3. Optical coherence tomography (OCT).** SD-OCT was performed with a *Spectralis* OCT system (Heidelberg Engineering, Heidelberg, Germany). Cross-sectional images were taken in the periphery as well as in the center of the device, if possible. *En-face* images were taken using confocal infrared imaging with a wavelength of 715 nm.

**2.4.4. Ultrasound imaging.** Ultrasound imaging was performed with a 10 Mhz B-scanning probe (Aviso S, Quantel Medical, Cournon d'Auvergne Cedex, France). It was used in cases of severe corneal edema or vitreal haemorrhage to evaluate the position of the VLARS and possibly identify retinal detachment and tearing, respectively.

After the last follow-up examination, euthanasia was induced using an overdose of a 2 mg kg<sup>-1</sup> dose of a barbiturate

(Narcoren, Merial GmbH, Hallbergmoos, Germany). Death was confirmed both clinically and by electrocardiographic monitoring.

## 2.5. Histology

**2.5.1. Hematoxylin and eosin staining.** Histology was performed as described by Rösch *et al* [16]. After enucleation, the eyes were fixated, punctured and immersion fixated for 30 min using 4% *paraformaldehyde* (PA) in 0.1 M phosphate buffer (PB) at room temperature. A tissue dehydration automat (mtm, Slee, Mainz, Germany) was used to dehydrate the ocular tissue using a series of increasing ethanol concentrations (twice with 70%, twice with 96%, three times with 100%, one hour each), followed by *xylene* (three times in one hour) and *paraffin* (four times in one hour). Prior to the next steps of histological preparation, the VLARS and the retinal tack were carefully removed after performing a circular incision in the anterior segment of the eye. The ocular tissue was embedded in *paraffin* and cut in sections of 5  $\mu\text{m}$  thickness using a microtome (Jung GMBH, Heidelberg, Germany). The position was chosen to capture tissue beneath the VLARS. After deparaffinization and rehydration, standard *hematoxylin* and *eosin* staining ensued. The images were taken using a microscope with an integrated image capturing system (Leica DMRX microscope, Leica Biosystems, Wetzlar, Germany).

**2.5.2. Resin embedding and thin-grind cutting.** Five eyes were prepared for an embedding in the plastic *Technovit 7200 VLC* for thin-grind cutting at the location of retinal tack protrusion. *Technovit 7200 VLC* (Kulzer GmbH, Hanau, Germany) is a one-component adhesive based on *glycolmethacrylat*. Fixation of the eyes was performed as described above. For infiltration of the tissue a 1:1 mixture of alcohol and *Technovit 7200* (Kulzer GmbH, Hanau, Germany), followed by pure *Technovit 7200* was used in a light-proof container. The posterior segment of the eye including the array and retinal tack were embedded parallel to the plane of interest into the embedding mould of the *Technovit* system. The area to be examined was facing downwards, the entirety of the tissue was covered in *Technovit 7200* without trapping air or elevating the tissue from the base of the mould. Polymerization was done using low light intensity and temperatures below 40 °C, while light with a higher intensity was applied during the second stage to cause polymerization in the infiltrated tissue. Cutting and grinding of the embedded tissue was performed with the *EXAKT* tissue preparation devices (*EXAKT 300 CP*, *EXAKT 400 CS*, *EXAKT Advanced Technologies GmbH*, Norderstedt, Germany). Each slice of embedded tissue was fixated to an acrylic glass holder using the precision adhesive *Technovit 7210 VLC*. Each slice had a thickness of 100  $\mu\text{m}$ . Images were taken with a Leica DMRX microscope (Leica Biosystems, Wetzlar, Germany).

## 2.6. Surgery for acute stimulation experiments in rabbit eyes

The acute stimulation experiments were conducted in two pigmented *Chinchilla Bastard* rabbits. General anesthesia was obtained by *isoflurane* (Abbott GmbH & Co. KG, Wiesbaden,

Germany) at 4% and maintained at 2% to 2.5%. The animals were intubated with a 2.5 mm tracheal tube (Rüsch, Rüschelit® Super Safety Clear, Sulzbach, Germany). For analgesia, a perfusion of *fentanyl* 0.5 mg ml<sup>-1</sup> (*fentanyl* 0.5 mg-rotexmedica, ROTEXMEDICA GmbH Arzneimittelwerk) at 0.1 ml h<sup>-1</sup> to 0.7 ml h<sup>-1</sup> was preserved.

During surgery the animals were fixated in a stereotactic frame. The points of contact of the frame and the animal's head were anesthetized with a subcutaneous injection of *bupivacainehydrochloride* 0.5% (*Bupivacain-RPR-Actavis* 0.5, Actavis, Luxemburg). To assess the VLARS' capability to elicit cortical responses upon electrical epiretinal stimulation, a 32-channel silicone probe for cortical recording - consisting of four shanks with eight electrodes arranged linearly on each shank (figure 6(A))—was carefully advanced into the V1 visual cortex (E32-150-S4-L10-10.5-1400-1200, ATLAS Neuroengineering, Leuven, Belgium) after a craniotomy over the area of interest was performed. The iridium oxide recording electrodes used for cortical recordings have a diameter of 35  $\mu\text{m}$ . The length of the shafts is 10.5 mm and 10 mm for the inner two and outer two respectively. The pitch of the shafts is 1.2 mm and 1.4 mm for the inner two and outer two respectively. Each shaft has eight electrodes starting from the tip with an inter-electrode distance of 150  $\mu\text{m}$ . The four shafts have a width of 140  $\mu\text{m}$  and a thickness of 50  $\mu\text{m}$ . Reference and ground of the recording system were connected to a silver wire that was placed at the edge of the craniotomy. The silver wire and the craniotomy were covered with low melting point agarose (4% in Ringer solution, Sigma Aldrich, Darmstadt, Germany) to prevent dehydration of the neocortex.

After obtaining cortical responses upon visual stimulation by a light flash, the cortical recording electrode was temporarily removed. The animals were then rotated out of the recording position so that the eye was positioned suitable for vitreoretinal surgery underneath a microscope (Zeiss Model OPMI 6-CFR XY, S5 Tripod, Carl Zeiss AG, Jena, Germany).

The vitreoretinal surgery was performed following the protocol established for the semi-chronic implantation as described above, except changing the 20 G ports to a 23 G port system.

Prior to inserting the active VLARS, the anterior chamber was filled with a viscoelastic fluid (*Healon*, Johnsen and Johnson, New Brunswick, USA) and the corneal incision was enlarged to 5 mm. Then, the array was advanced into the anterior chamber with the cable connector for the stimulator resting in the incision. The incision was sutured with two *Vicryl 6-0* sutures (Alcon, Wort Worth, USA). Subsequently, the active VLARS was advanced on top the PFCL phase on the posterior retinal pole. The PFCL was carefully removed and the implant was lowered towards the retinal surface. The residual PFCL was removed to prevent isolating effects. During the acute stimulation experiment, the VLARS was not fixated using retinal tacks to reduce the risk of retinal damage.

For the following air tamponade, the air pressure was set to 30 mm Hg with the vessels at the optic disk clearly perfused. After fixation of the connector cable at the stereotactic frame the animal was gently rotated back to the recording position. Afterwards, the correct position of the implant was confirmed

by indirect funduscopy with a 20D lens (Volk Optical Inc., Mentor, USA).

After finalization of the acute stimulation and recording experiments, the animals were sacrificed by a lethal dose of *fentanyl* 0.5 mg ml<sup>-1</sup> (fentanyl 0.5 mg-rotexmedica, ROTEXMEDICA GmbH Arzneimittelwerk).

### 2.7. Cortical recordings in an acute stimulation setting

During stimulation, up to 24 electrodes on the VLARS were active. In the experiment displayed here, electrodes of two clusters were used: the blue cluster (figure 6(B), blue circle S1) contained four active electrodes, while the red cluster (figure 6(B), red circle S2) contained nine active electrodes. A biphasic stimulation pulse repeated three times with 90  $\mu$ A per electrode in the blue cluster and 80  $\mu$ A per electrode in the red cluster for 200  $\mu$ s at a frequency of 200 Hz was chosen.

Data were acquired with a *Multichannel USB* recording system (ME32-FAI- $\mu$ PA-System, Multi Channel Systems, Reutlingen, Germany) and digitized at 25 kHz.

To obtain local field potentials (LFPs), data were down-sampled to 5 kHz and low-pass filtered (Butterworth, 2nd order, 300 Hz cutoff frequency) using *MC\_Rack* software (Multichannel Systems MCS GmbH). LFPs were averaged across all trials with *Spike2* software (Cambridge Electronic Design). To assess, if LFP responses to the stimulus were significant, baseline activity was measured 100 ms before stimulus onset and compared to responses 0.012 s to 0.15 s after stimulus onset (paired *t*-test, Bonferroni-corrected; Microsoft XLSTAT). To determine if retinal stimulation elicited differential responses in different recording locations, responses were first normalized to the absolute value of the response amplitude within each data set. Then response amplitudes were determined as the minimum values during a 0.012 s to 0.15 s window after stimulus onset and compared across stimulation conditions (unpaired *t*-test, Bonferroni-corrected).

## 3. Results

### 3.1. Implantation surgery and handling of the device in cadaveric porcine eyes

The implantation of the VLARS in cadaveric porcine eyes had the purpose to establish a regimen for the implantation in the *in vivo* biocompatibility study with suitable duration and a high safety level. Up to the actual implantation of the VLARS, the techniques applied did not exceed techniques of standard vitreoretinal surgery. Cadaveric porcine eyes beneficially share an equal size with human eyes and in the cadaveric surgery, bleeding and the development of proliferative membranes as seen in porcine eyes after *in vivo* surgery have not to be considered [17].

Additionally, the best method of safely introducing the large array into the eye had to be discovered and tested. Ideally, the array is folded to temporarily reduce its surface area, thus decreasing the size of the corneal incision to the diameter of the implantation cone's most anterior segment (approx. 5 mm). The star shaped array folded concentrically,

while the globe shaped stimulator was rolled up. The arrays were advanced using the retinal tack holder or surgical forceps with silicone tips suitable for handling electrical devices (Geuder AG, Heidelberg, Germany). During surgery, it became obvious, that the globe shaped array did not properly fold as expected, thus leading to an uncontrolled opening and difficult handling inside the implantation cone and the anterior segment of the eye, respectively. Figures 2(D)–(F) shows the process of introducing the globe shaped array into the anterior chamber. As seen in figures 2(E) and (F), the globe shaped VLARS does not fold concentrically. These findings lead to abandoning the globe design in later stages of this study. The insertion of the star shaped array by using the implantation cone is depicted in figures 2(G)–(I). Being able to fold the star shaped structure concentrically proved to be a major advantage over the globe shaped array granting easier handling and a controlled passage into the anterior chamber.

In cadaveric porcine eyes, corneal opacity depends on the duration between enucleation and beginning of the surgery. In our study, we did not encounter severe corneal opacity. Lensectomy and *pars-plana* vitrectomy were conducted in a suitable duration and did not cause adversities. Insufficient suturing and an overly wide corneal incision caused low intraocular pressure in some cases. Reduced composure of the eye can lead to choroidal swelling in an *in vivo* setting and to premature contact of the array with the retinal surface.

Overall, our group introduced an implantation surgery, which could be transferred to the semi-chronic *in vivo* study in rabbits.

### 3.2. Feasibility and safety of the implantation procedure in the implantations in rabbits

In the *in vivo* implantation study in rabbits, safe handling and retinal fixation of the array rendered to be the most challenging aspects. Table 1 collects the results of the implantation surgeries and the results gathered during the follow-up period. The most important findings concerning surgical feasibility and the follow-up examinations are summed up in the next paragraphs.

In the first implantation, the corneal incision applied for the phacoemulsification was enlarged to approximately 10 mm. Thus, enabling better mobilization of the cone and the VLARS yet causing a loss of ocular stability. The implantation cone did not prove to be significantly beneficial compared to the use of the surgical instruments directly inserting the array through the corneal incision. By using these instruments, the corneal incision did not have to be further enlarged from the initial 5 mm, thus granting a better ocular composure, shorter time of implantation and easier handling. The implantation cone was ultimately abandoned after the first *in vivo* implantation.

Positioning and fixation of such large stimulating arrays into rabbit eyes were challenging. In six of the ten rabbits a stable epiretinal position at the posterior pole could be achieved at the end of the surgery using the central aperture for the retinal tack. In three subjects it was not possible to use the central tack aperture (aperture was located directly over the optic disc/aperture was ripped during implantation

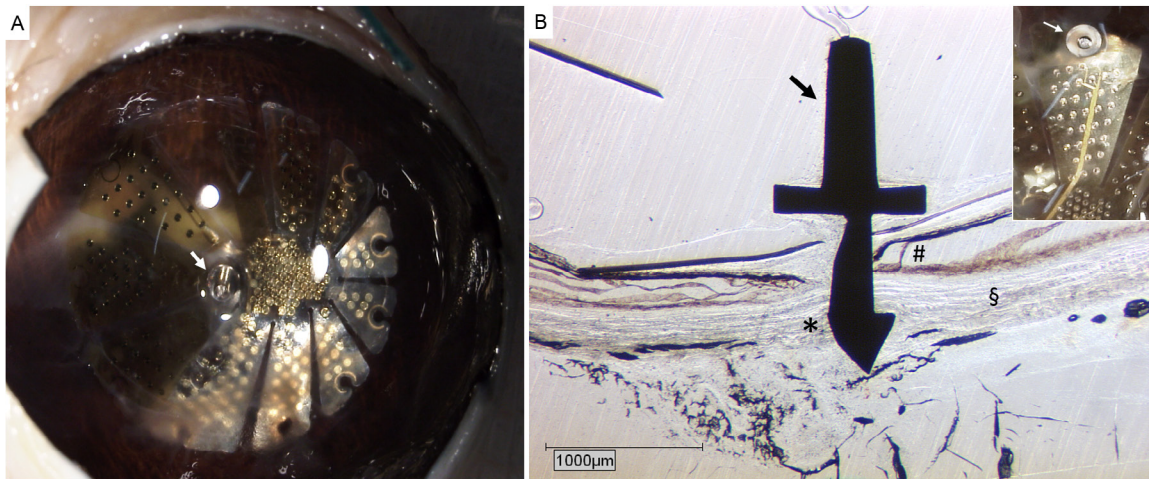


**Figure 4.** Open-sky imaging and *epoxy-resin* embedding. (A) (Animal 1): open-sky imaging of the VLARS. The white arrow indicates the central position of the retinal tack. The enucleation took place 12 weeks after the implantation. (B) (Animal 7): *Epoxy-resin* embedding of the retinal tack and the VLARS on the retina. The *epoxy-resin* embedding took place 12 weeks after implantation. The retinal tack (black arrow) protrudes into the sclera. In this eye, a peripheral aperture was used to insert the retinal tack (top right picture, the white arrow indicates the retinal tack). The diamond sign indicates the space between the VLARS array above and the retina beneath. The paragraph sign indicates the sclera. The asterix indicated moderate scar tissue around the penetrating area of the retinal tack.

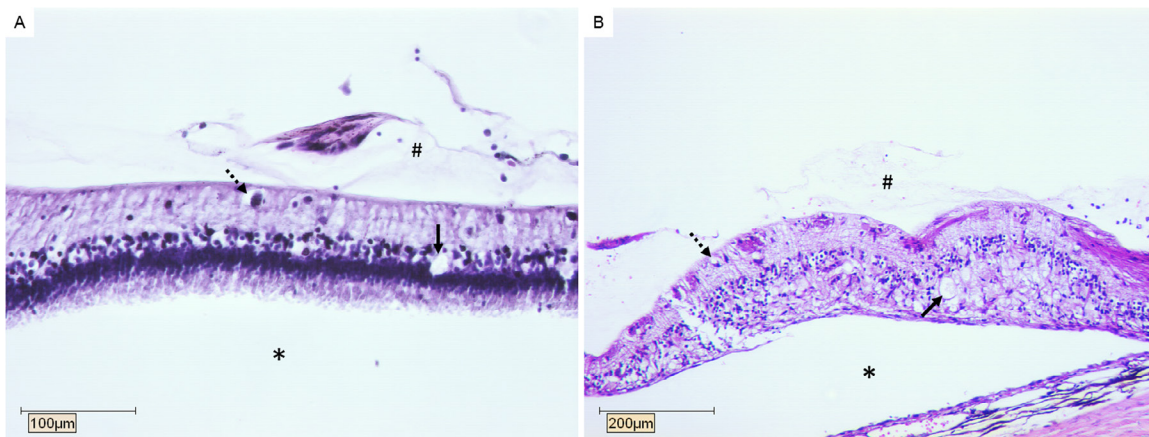


**Figure 5.** *Hematoxylin* and *eosin* staining 12 weeks after implantation. (A) (Animal 1): the histological section depicted was located underneath a wing of the star shaped VLARS. The section shows moderate vacuolization in the inner nuclear layer (dashed arrow) and the outer nuclear layer (arrow), as well as preretinal gliosis (diamond sign). The layers of the retina are intact. (B) (Animal 1): the histological section depicted was located closely to the center of the star shaped VLARS. The section shows moderate vacuolization in the inner nuclear layer (dashed arrow) and the outer nuclear layer (arrow), as well as preretinal gliosis (diamond sign). Note the degeneration of the retinal structure, presumably caused by a retinal detachment. In both sections, the subretinal space is marked with the asterix.

procedure), which resulted in fixating the array with two peripherally placed tacks in one animal (animal 6), and one peripherally placed tack in two animals (animals 4 and 7). In two of these subjects (animals 4 and 6), the array was not fixated sufficiently at the end of the implantation surgery, yet the study was continued to examine the effects on the eye. In one animal, the central retinal tack did not grant epiretinal fixation (animal 10). During the fourth week follow-up examination of this animal, severe retinal detachment, as well as a complete dislocation of the array were detected, leading to the immediate termination of the follow-up and euthanasia.

Primary retinal detachment and retinal tears were observed as severe adverse events. These occurred in five of ten rabbits in varying severity (table 1). Retinal tears were caused by the sharp edges of the large arrays harming the retina either during positioning of the array at the posterior pole or during

phases of hypotony with temporary involution of the eye. Out of these cases, two animals (animals 4 and 10) experienced a larger retinal detachment, while three animals (animals 5, 6 and 7) experienced focal retinal tearing. In one animal, the accidental contact of the infusion with the opposing retinal surface during a period of low intraocular pressure caused severe retinal tearing and eventually retinal detachment (animal 10).

Intravitreal bleeding varied in its severity, yet noteworthy bleeding occurred in three eyes (animals 3, 6, and 7). The bleeding was staunched in all cases and did not jeopardize the ongoing implantation. One eye (animal 4) suffered from subretinal hemorrhage. One eye (animal 9) suffered from a choroidal detachment, which vanished over the course of the follow-up.

Using PFCL as a liquid cushion to support the stimulator seemed mandatory in order to avoid uncontrolled movement

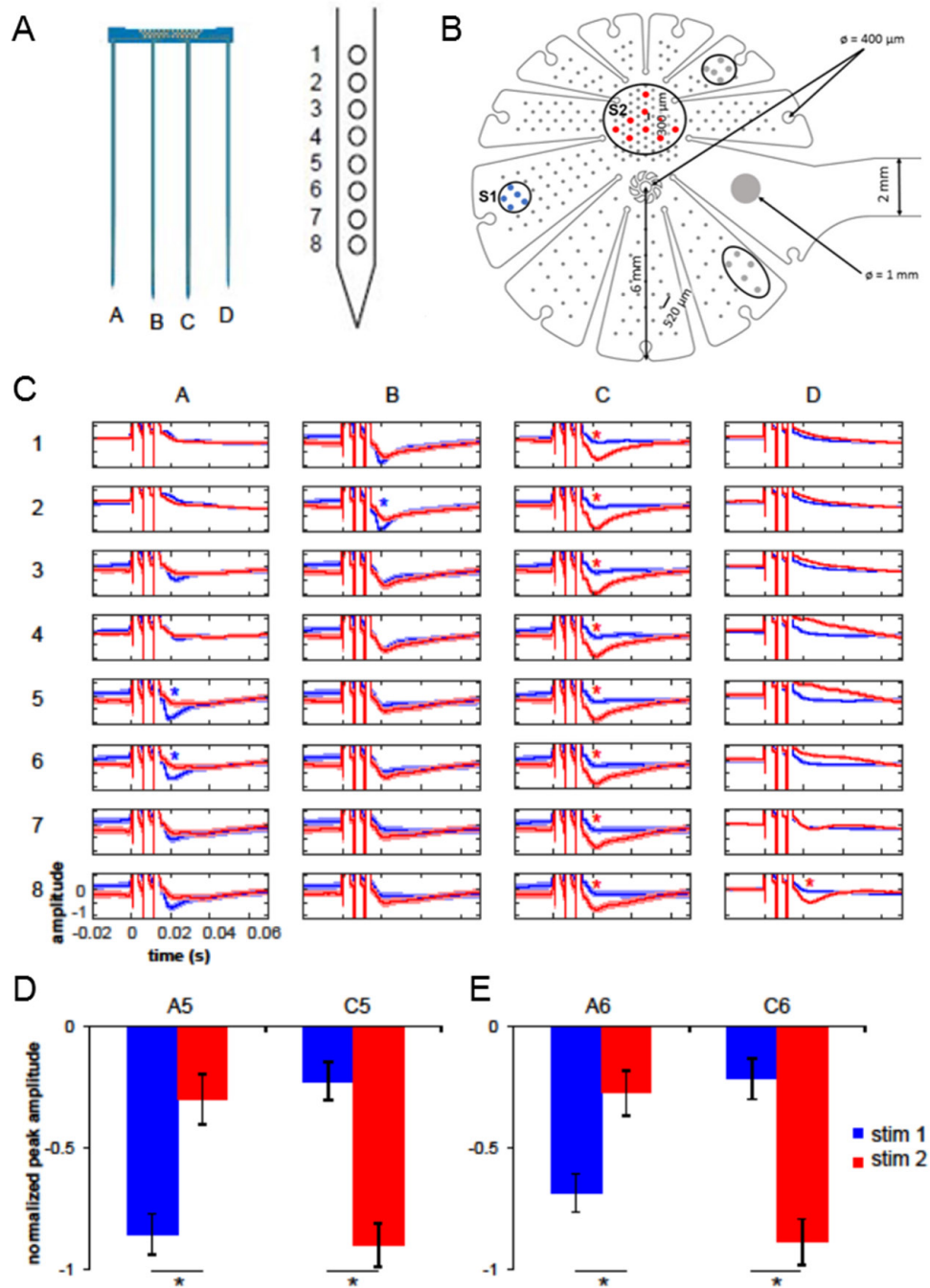


**Figure 6.** Retinal stimulation evokes LFP responses in rabbit primary visual cortex (V1) A: Schematic of the 32-channel silicone probe inserted in V1 in the rostro-caudal direction ((A)–(D) shanks; (A), left side). Each shank comprises eight electrodes spanning cortical layers 1 to 6 ((A), right side). (B) Schematic design of the star shaped VLARS-design. The connecting cable has a width of 2 mm, the radius measured from the central aperture is 6 mm. The apertures in the center and in the periphery have a diameter of 400  $\mu\text{m}$ . The single return electrode has a diameter of 1 mm (large grey electrode), the other electrodes have a diameter of 100  $\mu\text{m}$  (not shown in figure). Note that the distance between the electrodes varies based on their position (approx. 520  $\mu\text{m}$  on the wings versus 300  $\mu\text{m}$  in the center); The electrode cluster S1 consists of five active electrodes. The electrodes are highlighted in blue, and represent the corresponding cortical responses to stimulus 1 (blue traces) in (C)–(E). The electrode cluster S2 consists of nine active electrodes. These electrodes are highlighted in red, and represent the corresponding cortical responses to stimulus 2 in (C)–(E). The remaining two encircled electrode clusters consist of 5 active electrodes each. (C) Normalized response amplitudes to stimulus 1 (blue traces) and stimulus 2 (red traces) for each electrode (horizontal: shanks (A)–(D), vertical: electrodes 1 to 8). Following stimulus onset at time 0s, three stimulation artifacts are visible before stimulus-evoked responses emerge as negative deflections. Blue and red asterisks indicate significantly larger responses to stimulus 1 and 2, respectively (unpaired *t*-test, Bonferroni-corrected). Shaded error bars indicate the standard error of the mean (SEM). (D) and (E) Examples demonstrating the reversal of response magnitudes during stimulation. Stimulus 1 (blue) elicited a greater response at electrode A5 compared to C5, while stimulus 2 (red) evoked a larger response at C5 than A5 (unpaired *t*-test, Bonferroni-corrected; panel D). Similarly, stimulus 1 elicited a stronger response at electrode A6 than C6, while stimulus 2 did the reverse (unpaired *t*-test, Bonferroni-corrected; panel E).

**Table 1.** Results of the semi-chronic implantation of the VLARS in ten rabbits.

Animal	Method of implantation	Retinal tack/tack fixation during implantation	Adverse events during surgery	Follow-up	Fundus imaging	OCT-imaging	Open-sky imaging
1 CB flat VLARS	Cone	Central/stable	Moderate (difficulty retracting PFCL from underneath the array)	Moderate adverse events (corneal edema, retinal penetration of array)	Bad visibility from weeks 2 to 7	Partly distant to retinal surface, partly protruding into the retina (figures 3(B)/(C))	Array fixated, mild gliosis beneath array (figure 4(A))
2 A flat VLARS	Cannula, push-pull manipulator	Central/stable	Mild (mild choroidal bleeding)	Mild adverse events (slight retinal penetration of array, gliosis)	Good visibility (figure 2(E))	Epiretinal position in week 1 (figures 3(A)/(D))	Array fixated, mild gliosis beneath array
3 A flat VLARS	Cannula, anatomical forceps	Central/stable	Mild (mild intravitreal bleeding)	mild adverse events (slight retinal penetration of array, gliosis) <sup>c</sup>	Good visibility <sup>c</sup>	Epiretinal alignment <sup>c</sup>	Array fixated, wings adjacent to retinal surface <sup>c</sup>
4 A flat VLARS	Tear duct probe	Central <sup>a</sup> and peripheral/dislocation of central tack, unstable fixation	Severe (subretinal/choroidal bleeding, phacoemulsification malfunction causing corneal damage, retinal tearing adjacent to array, dislocation of central tack due to tear in central aperture)	severe adverse events (severe edema with vascularization, intravitreal bleeding, dislocation of retinal tack, hyphema)	Bad visibility over course of 12 weeks due to corneal edema and vitreal bleeding	Array partly distant to retinal surface, week 12: bubble of heavy liquid beneath array	Array fixated, retinal protrusion, gliosis
5 A flat VLARS	Rhexis forceps	Central/in position, slightly loose	Moderate (retinal tearing adjacent to array)	mild adverse events (moderate injection of conjunctiva)	Good visibility (figure 3(F))	Low quality	Array fixated, wings distant to surface, gliosis
6 A flat VLARS	Tear duct probe	Two peripheral nails/dislocation of one tack, unstable fixation	Moderate (use of two tacks, mild vitreal bleeding, peripheral retinal detachment)	Moderate adverse events (corneal edema, low IOP, shallow anterior chamber)	Bad visibility after first week due to vitreal bleeding	Week 8: array partly distant to retinal surface	Bad fixation, only one peripheral tack, gliosis
7 CB flat VLARS	Anatomical forceps	One peripheral tack <sup>b</sup> /stable	Moderate (vitreal bleeding after inserting first peripheral tack, dislocation of peripheral tack, retinal tearing adjacent to array)	Moderate adverse events (severe corneal edema, slight retinal penetration of array, gliosis, retinal wrinkling)	Good visibility	Low quality	Array fixated, peripheral tack, 1/3 of wings distant to retinal surface

(Continued)

**Table 1.** (Continued)

Animal	Method of implant-ation	Retinal tack/tack fixation during implantation	Adverse events during surgery	Follow-up	Fundus imaging	OCT-imaging	Open-sky imaging
8 CB flat VLARS	Tear duct probe	Central/initially stable	Mild (relatively large corneal incision)	Severe adverse events (severe edema with vascularization, fibrinous reaction anterior chamber, hyphema, dislocation of retinal, retinal bleeding, tack dislocation?)	Bad visibility through course of 12 weeks	Low quality	Array not fixated, gliosis
9 A curved VLARS	Anatomical forceps	Central/stable	Mild (choroidal detachment)	Mild adverse events (slight vitreal bleeding during the first week after implantation)	Bad visibility in week 1 due to vitreal bleeding	Low quality, capture part of the array distant to retinal surface	Array fixated, coagulated hemorrhage on array
10 CB curved VLARS	Anatomical forceps	Central/dislocation of entire array, yet tack in central aperture	Moderate (infusion caused tearing of peripheral retina during period of hypotony, retinal tack repositioned multiple times)	Severe adverse events (complete retinal detachment) <sup>d</sup>	Good visibility <sup>d</sup>	Low quality, capture part of the array distant to retinal surface	Array not fixated <sup>d</sup>

CB: Chinchilla bastard rabbit.

NW: New Zealand White rabbit.

<sup>a</sup> Central tack dislocated during implantation surgery.

<sup>b</sup> : Second peripheral tack dislocated during implantation surgery.

<sup>c</sup> Animal died during anesthesia at the four week follow-up examination.

<sup>d</sup> Termination of follow-up due to complete dislocation of the epiretinal array.

of the device within the globe although removing the PFCL bubble from underneath the array was difficult and time consuming. Tangential movements of the stimulator put the retina at risk for retinal tears. Overall, the implantation procedure is feasible, yet challenging on different levels. The mean duration for the implantation surgery was approximately two hours, decreasing over the course of the study.

### 3.3. Clinical follow-up in the semi-chronic implantation in rabbits

Clinical follow-up over 12 weeks could be achieved in eight of ten animals. In two animals, the follow-up phase was terminated after four weeks: one animal died in anaesthesia during the control examination (animal 4), the follow-up of the other animal was terminated because of a severe retinal detachment and dislocation of the VLARS, as mentioned above (animal 10).

Throughout the 12-week follow-up period, no significant intraocular inflammation or endophthalmitis was observed. One animal showed a fibrinous reaction and hyphema after implantation, in addition to a severe corneal edema (animal 8). Another animal showed epithelial vascularisation and a severe corneal edema (animal 4).

Overall, significant corneal edema with tendency to clear over time occurred in five rabbits (animals 1,4,6,7 and 8), with three cases of a severe edema likely due to the relatively large corneal incision (animals 4, 7 and 8). Treatment of the edema consisted of an ointment of 1 g of *hydrocortisone-acetate* and *glucose 70%* (HCG-Augensalbe. Pharmacy of the RWTH Aachen University, Germany). The edema disappeared gradually under treatment, yet it highly interfered with funduscopy, fundus photography and OCT-imaging in the follow-up examinations.

The quality of OCT-imaging was not only reduced by the opacity of the cornea, but also by diffuse reflection of the array's surface, the gold wiring and electrodes, respectively. Depending on the condition of the cornea, analysis of epiretinal alignment during the follow-up phase was therefore conducted by using summarized information of all analyzing methods: funduscopy, OCT and ultrasound imaging.

The overall analysis of epiretinal alignment during the complete clinical follow-up can be categorized in three categories: good (complete to 2/3 contact of the stimulator), medium (2/3 to 1/3 contact of the stimulator) and poor (<1/3 contact of the stimulator). Good epiretinal contact could be achieved in two animals (animals 2 and 3 [until premature death]), medium in four animals (animals 1,4,7 and 9) and poor in four animals (animals 5,6, 8 and 10). Overall, epiretinal alignment turned out to be good even after surgical complications, as well as be poor due to later complications during the follow-up period.

Figures 3(A)–(D) depicts four observations obtained with OCT-imaging in two animals at different time points. While figure 3(A) shows proper alignment in the periphery, the array is distant to the retinal surface in figure 3(B). Figure 3(C) shows protrusion of the array into the retina in the same animal, while in figure 3(D) the retina experiences stress under the radial pressure of the array.

In figures 3(E)–(F), fundus photography 12 weeks after implantation in two animals is shown. The retinal tack is observable in the central aperture. Note the difference in reflectance hinting to varying alignment to the retinal surface.

### 3.4. Open-sky imaging and histological analysis

Prior to the histological staining and resin embedding, open sky imaging was performed. This allowed us to determine the retinal fixation of the VLARS and possible damage on the retina. Figure 4(A) shows good epiretinal positioning of a star shaped VLARS. The retinal tack is positioned in the central aperture. The results obtained from the open sky examination varied. After 12 weeks, five out of the ten implanted eyes showed insufficient fixation of the VLARS and dislocation of the retinal tacks. In one eye, retinal detachment was observed, which had not been seen during the implantation surgery or the follow-up. However, it is not clear, if dislocation of either tack or the VLARS could possibly be caused by the preceding treatment for histological staining or the traumatic opening of the eye.

Figure 4(B) shows the result of grinding the embedded eye upon the section of the tack penetrating the retina. In this implantation surgery, the tack was inserted into a peripheral aperture (figure 4(B), top right corner). The tack protrudes intentionally into the eye's sclera as its desired position. Moderate scar tissue is found around the retinal penetration as indicated by the asterisk in figure 4(B). The findings were also observable in the other eyes which underwent resin embedding (data not shown).

Figure 4 depicts the *hematoxylin* and *eosin* staining 12 weeks after implantation. The sections shown in figure 5(A) was taken from underneath a wing of a star shaped array, while the section in figure 5(B) is taken from underneath the array's center.

Both sections show moderate vacuolization, predominantly in the outer and inner nuclear layer. In figure 5(A), no signs of inflammation or cellular migration can be observed. The layers of the neurosensory retina seem intact, the shown detachment is likely caused by the preceding fixating treatment. In figure 5(B), the retinal structure seems disturbed, the retinal layers are degenerated, compatible to histological findings in retinal detachment. While in open-sky imaging retinal detachment was not decisively observable, preretinal gliosis was found underneath the array. The findings are consistent in the obtained sections of other implanted eyes (data not shown).

### 3.5. Findings of the implantation surgery in the acute stimulation

The acute stimulation experiments took place after the implantation surgeries of the ten rabbits were concluded, thus the protocol was refined and the surgical tools were established.

Switching to a valved 23 Ga port system for the pars-plana vitrectomy did not cause any adverse effects but instead seems to give a greater stability of the eye pressure during the procedure.

To grant a stable position of the animal in the acute stimulation experiment the animals are fixated in a stereotactic frame. This set-up allowed us to safely maneuver the animal back and forth from a position suitable for retinal stimulation and cortical recording to a position suitable for surgery. Any movement after implantation of the VLARS had to be done with great caution since the epiretinal VLARS was not fixated with a retinal tack as in the semi-chronic implantation. Lacking any form of physical fixation, close epiretinal alignment was solely granted by the success of the implantation, and especially the careful removal of the PFCL bubble beneath the array. Using any form of heavy liquid (i.e. PFCL, silicone oil) was discarded due to their isolating properties, thus prohibiting retinal stimulation.

Another important difference to the semi-chronic implantation surgery was the presence of a connector cable leading to the stimulator unit outside the eye positioned at the corneal incision. A permanent aperture in the anterior segment of the eye would lead to a temporary instability of the eye. Adding multiple *Nylon 10-0* sutures (Alcon, Fort Worth, USA) to the corneal incision eventually granted stability.

Overall, safely maneuvering the animal as well as the lack of physical fixation added further challenges to the implantation surgery, yet in the two cases a successful implantation was achieved and the acute stimulation and recording was performed.

### 3.6. Cortical recordings in acute epiretinal stimulation

The cortical recording electrode and one of its shanks are shown in figure 6(A). After the craniotomy, we were able to record cortical potentials elicited by bright light stimulation to verify the electrode's correct position. Figure 6(B) shows the schematic design of the star shaped VLARS illustrating the distribution of active electrodes, as well as giving a detailed insight in the array's measurements. Figure 6(B) shows the active electrode clusters encircled, the active electrodes are graphically enlarged and colored corresponding to the stimulus. The active electrode clusters used in the acute study shown below are highlighted in blue for stimulus 1 (figure 6(B) and S1) and red for stimulus 2 (figure 6(B) and S1). Figures 6(C)–(E) give an overview of the results obtained during the acute stimulation experiments in one of the two tested rabbits.

The normalized response amplitudes in figure 6(C) demonstrate a different cortical response pattern corresponding to the varying area of stimulation on the retina. The blue and red asterisks indicate significantly larger responses to stimulus 1 and 2, respectively. Looking at individual electrodes with seemingly high responses the assumption above is further supported. Figures 6(D) and (E) compare electrodes from shank (A) and (C), showing that the recorded LFPs are significant to both clusters of stimulation, yet significantly higher for shank A when stimulation occurred with electrodes in the blue cluster or in shank (C) when stimulation occurred with electrodes in red cluster. Thus, we were able to demonstrate the VLARS' ability to elicit reproducible cortical responses

corresponding to epiretinal stimulation in distant areas of the retinal surface.

## 4. Discussion

The concept study was aiming at introducing an epiretinal stimulator capable of stimulating a wider aspect of the retinal surface than any other currently available stimulators, thus creating a meaningful visual field. We chose the epiretinal pathway due to our group's experience in this field as well as the overall positive feedback received from the commercially available epiretinal stimulator system *ARGUS II* [17–20].

Besides the obvious complexity of engineering such microsystems, the major obstacle was a feasible and safe implantation procedure. Altering the method of inserting the array into the anterior chamber by using various standard tools pathed the way for a less timely and safer implantation. In the acute setting we decided to refrain from retinal fixation via a retinal tack to spare the retina from the additional risk of tearing and detachment. This was suitable since the experiment was performed in general anesthesia and in a stereotactic apparatus hindering any uncontrolled movement.

Corneal edema, intravitreal bleeding and insufficient fixation of the arrays were the main impairments during and after semi-chronic implantation surgery. Especially retinal detachment and tearing, as well as safe and sufficient fixation of the array were threatening the success in various subjects as detailed above. Over the course of the study, our group was able to improve the implantation procedure, yet using retinal tacks to fixate the array on the retinal pole remains unsuitable. It is crucial to consider the different dimensions of the rabbit's eye compared to those of humans, or pigs, on which prior implantation experiments were performed [17, 21, 22]. The VLARS was developed with the human eye in mind, yet the design of the experiment and the legislation on animal experiments made the use of a smaller animal more suitable. We expect, that the implantation of the VLARS in a human eye would be less traumatic for the retina. The observations gathered during the follow-up period gave a mixed image of success, but also failure as shown above.

Calculations have shown, that our VLARS device's 250 electrodes cover a possible visual field of  $18.8^\circ$ , corresponding to a visual angle of  $37.6^\circ$  [14]. According to the work of Dagnelie *et al*, a visual angle of  $27^\circ$  consisting of a  $16 \times 16$  pixel matrix is the threshold for navigating safely through a given environment [13]. In theory the VLARS structure fulfills this requirement. To do reading tasks efficiently, Cha *et al* claim that 625 pixels on a 10 mm by 10 mm matrix are necessary [23]. This would theoretically grant a visual acuity of 20/30 far surpassing the capabilities of any current retinal stimulator. The proclaimed necessity of a central visual acuity of 20/80 to perform pattern recognition tasks by Palanker *et al* demands about 18 000 individual pixels on an array of 3 mm in diameter [24]. This further demonstrates the gap between the requirements of a retinal stimulator and the current technical as well as physiological feasibility. The 250 electrodes mounted on the VLARS do not match those requirements either although

surpassing the 60 electrodes of the epiretinal *ARGUS II* device by a large margin. Additionally, creating a significantly larger epiretinal array did not have the intention of improving central acuity significantly, yet adding meaningful visual field. The changing distribution, as depicted in figure 6, with an electrode pitch of 300  $\mu\text{m}$  in the central 2.5 mm<sup>2</sup> of the array and a pitch of 520  $\mu\text{m}$  on the peripheral wings further underlines this aspect.

Implanting particularly large retinal stimulators has been the goal of different other groups as well, yet the focus was mainly laying on suprachoroidal implantation. Villalobos *et al* designed a single array for suprachoroidal implantation measuring 19 × 8 mm and mounting 21 electrodes. The array is implanted into a rather large scleral pocket with an opening close to the corneal limbus. Their studies conclude that implantation is safe and feasible, and the array elicits cortical activation via suprachoroidal stimulation [25, 26]. This approach was further pursued by Abbott *et al*, members of the same group, by increasing the number of electrodes to 44 on a silicone carrier about the same size (17 × 8.5 mm) as the one used by Villalobos [25, 27]. Results from a chronic passive implantation showed promising results [27]. Comparable to that approach, Lohmann *et al* tested a dual-array suprachoroidal stimulator with a size of 5.18 mm × 5.18 mm for each of the arrays, mounting up to 50 electrodes in total theoretically (25 electrodes on each of the two arrays) [28]. A safe implantation procedure was shown in their work, as well as chiasma responses and changes in the reflectance caused by trans-choroidal stimulation. Suprachoroidal implantation seems feasible for larger arrays because intraocular surgery is not necessary nor any kind of fixation on the retinal surface. Using a scleral pocket, the suprachoroidal array is aligned to the eye inherent curvature [29]. However, compared to epiretinal and subretinal stimulation, suprachoroidal stimulation systems have a major disadvantage concerning the visual acuity. The highest accessible visual acuity of suprachoroidal systems seems significantly inferior to those shown in epiretinal and subretinal systems with an acuity of 20/4451 in the suprachoroidal system developed by Ayton *et al* versus 20/1262 in the epiretinal *ARGUS II* or even 20/200 in the subretinal *alpha-IMS* [20, 30, 31]. Especially the *Alpha-IMS* surpasses other approaches of prosthetic vision in terms of sheer electrode number by a large margin with 1500 individual electrodes, yet ultimately creating a 38 × 40 pixel matrix granting a visual angle of 11° by 11° [30]. Thus, surpassing epiretinal systems in theoretical visual acuity, the size of subretinal systems is limited by the method of implantation [24, 32]. By implanting multiple subretinal photovoltaic arrays, the *PIXIUM Vision SA PRIMA* system attempts to combine both high resolution of subretinal implants and the restoration of a large visual field. Currently, an interventional clinical trial including patients suffering from age-related macular degeneration, opposed to retinal dystrophies, is in progress (clinicaltrials.gov identifier: NCT03333954).

Sharing similar properties with the VLARS, the POLYRETINA is an approach introduced recently by Ferlauto *et al* [33]. The PDMS (*polymethylsiloxane*) based epiretinal array mounts 2215 photovoltaic stimulating pixels granting a theoretical visual angle of 46.3° and a theoretical restoration

of visual acuity of about 20/600. During the implantation procedure the flexibility of the POLYRETINA is used to concentrically fold the array and insert it over a scleral incision of about 6 to 7 mm very much like the implantation procedure shown in this work. Also, the POLYRETINA array takes a hemispherical shape to achieve a close alignment to the retinal surface, conquering a challenge displayed in our work. Curving the VLARS array prior to the implantation did not result in better properties for the retinal fixation in our study, though total surface area of the POLYRETINA surpasses the VLARS by a large margin, resulting in even greater challenges concerning epiretinal alignment. While showing promising results in implantation experiments in dummy and cadaveric eye, as well as demonstrating capabilities of stimulating rd10 mouse retina, the newly developed array has yet to prove itself in an *in vivo* setting [33].

## 5. Conclusion

Overall, our study showed the possibility of combining the beneficial properties of retinal stimulation of epiretinal systems shown in the past, and the possible recovery of meaningful peripheral vision. Along the primary implantation procedure and further testing different challenges occurred which could be dealt with as described above, yet especially retinal fixation of a very large epiretinal array remains an aim for future studies.

## Acknowledgment

Data and findings of this manuscript were partially shown at ‘The Eye and the Chip 2016’. The VLARS project was supported with a grant from the Jackstädt Foundation and with additional funding from the Hans Lamers Foundation. The authors thank Claudia Werner for her outstanding technical support.

Rudolph Pivik supported the VLARS team with the rotational stereotactic frame.

## ORCID iDs

Tibor Karl Lohmann  <https://orcid.org/0000-0003-4432-1853>  
 Florent Haiss  <https://orcid.org/0000-0001-8351-3685>  
 Florian Waschkowski  <https://orcid.org/0000-0001-7314-5022>

## References

- [1] Hartong D T, Berson E L and Dryja T P 2006 Retinitis pigmentosa *Lancet* **368** 1795–809
- [2] Kocur I and Resnikoff S 2002 Visual impairment and blindness in Europe and their prevention *Br. J. Ophthalmol.* **86** 716–22
- [3] Humayun M S *et al* 1999 Morphometric analysis of the extramacular retina from postmortem eyes with retinitis pigmentosa *Invest. Ophthalmol. Vis. Sci.* **40** 143–8

- [4] Lin T C *et al* 2015 Retinal prostheses in degenerative retinal diseases *J. Chin. Med. Assoc.* **78** 501–5
- [5] Humayun M S *et al* 1999 Pattern electrical stimulation of the human retina *Vis. Res.* **39** 2569–76
- [6] Rizzo J F III, Wyatt J, Loewenstein J, Kelly S and Shire D 2003 Perceptual efficacy of electrical stimulation of human retina with a microelectrode array during short-term surgical trials *Invest. Ophthalmol. Vis. Sci.* **44** 5362–9
- [7] Rizzo J F III, Wyatt J, Loewenstein J, Kelly S and Shire D 2003 Methods and perceptual thresholds for short-term electrical stimulation of human retina with microelectrode arrays *Invest. Ophthalmol. Vis. Sci.* **44** 5355–61
- [8] Lewis P M *et al* 2016 Advances in implantable bionic devices for blindness: a review *ANZ J. Surg.* **86** 654–9
- [9] Ghezzi D 2015 Retinal prostheses: progress toward the next generation implants *Frontiers Neurosci.* **9** 290
- [10] Rachitskaya A V and Yuan A 2016 Argus II retinal prosthesis system: an update *Ophthalmic Genet.* **37** 260–6
- [11] Gekeler K *et al* 2018 Implantation, removal and replacement of subretinal electronic implants for restoration of vision in patients with retinitis pigmentosa *Curr. Opin. Ophthalmol.* **29** 239–47
- [12] Geruschat D R, Turano K A and Stahl J W 1998 Traditional measures of mobility performance and retinitis pigmentosa *Optom. Vis. Sci.* **75** 525–37
- [13] Dagnelie G, Keane P, Narla V, Yang L, Weiland J and Humayun M 2007 Real and virtual mobility performance in simulated prosthetic vision *J. Neural Eng.* **4** S92–101
- [14] Waschowski F *et al* 2014 Development of very large electrode arrays for epiretinal stimulation (VLARS) *Biomed. Eng. Online* **13** 11
- [15] Waschowski F and Wilfried M 2017 Wide field epiretinal stimulator with adjustable curvature *SSI 2017: Int. Conf. and Exhibition on Integration Issues of Miniaturized Systems (Cork, Ireland March 2017)*
- [16] Rosch S, Johnen S, Muller F, Pfarrer C and Walter P 2014 Correlations between ERG, OCT, and anatomical findings in the rd10 mouse *J. Ophthalmol.* **2014** 874751
- [17] Menzel-Severing J *et al* 2011 Surgical results and microscopic analysis of the tissue reaction following implantation and explantation of an intraocular implant for epiretinal stimulation in minipigs *Ophthalmic Res.* **46** 192–8
- [18] Roessler G *et al* 2009 Implantation and explantation of a wireless epiretinal retina implant device: observations during the EPIRET3 prospective clinical trial *Invest. Ophthalmol. Vis. Sci.* **50** 3003–8
- [19] Keseru M *et al* 2012 Acute electrical stimulation of the human retina with an epiretinal electrode array *Acta Ophthalmol.* **90** e1–8
- [20] Ho A C *et al* 2015 Long-term results from an epiretinal prosthesis to restore sight to the blind *Ophthalmology* **122** 1547–54
- [21] Bozkir G, Bozkir M, Dogan H, Aycan K and Guler B 1997 Measurements of axial length and radius of corneal curvature in the rabbit eye *Acta Med. Okayama* **51** 9–11
- [22] Sanchez I, Martin R, Ussa F and Fernandez-Bueno I 2011 The parameters of the porcine eyeball *Graefe's Arch. Clin. Exp. Ophthalmol.* **249** 475–82
- [23] Cha K, Horch K and Normann R A 1992 Simulation of a phosphene-based visual field: visual acuity in a pixelized vision system *Ann. Biomed. Eng.* **20** 439–49
- [24] Palanker D, Vankov A, Huie P and Baccus S 2005 Design of a high-resolution optoelectronic retinal prosthesis *J. Neural Eng.* **2** S105–20
- [25] Villalobos J *et al* 2013 A wide-field suprachoroidal retinal prosthesis is stable and well tolerated following chronic implantation *Invest. Ophthalmol. Vis. Sci.* **54** 3751–62
- [26] Villalobos J *et al* 2014 Cortical activation following chronic passive implantation of a wide-field suprachoroidal retinal prosthesis *J. Neural Eng.* **11** 046017
- [27] Abbott C J *et al* 2018 Safety studies for a 44-channel suprachoroidal retinal prosthesis: a chronic passive study *Invest. Ophthalmol. Vis. Sci.* **59** 1410–24
- [28] Lohmann T K *et al* 2016 Surgical feasibility and biocompatibility of wide-field dual-array suprachoroidal-transretinal stimulation prosthesis in middle-sized animals *Graefe's Arch. Clin. Exp. Ophthalmol.* **254** 661–73
- [29] Ameri H, Ratanapakorn T, Ufer S, Eckhardt H, Humayun M S and Weiland J D 2009 Toward a wide-field retinal prosthesis *J. Neural Eng.* **6** 035002
- [30] Stingl K *et al* 2013 Artificial vision with wirelessly powered subretinal electronic implant alpha-IMS *Proc. Biol. Sci.* **280** 20130077
- [31] Ayton L N *et al* 2014 First-in-human trial of a novel suprachoroidal retinal prosthesis *PLoS One* **9** e115239
- [32] Yue L, Weiland J D, Roska B and Humayun M S 2016 Retinal stimulation strategies to restore vision: fundamentals and systems *Prog. Retinal Eye Res.* **53** 21–47
- [33] Ferlauto L *et al* 2018 Design and validation of a foldable and photovoltaic wide-field epiretinal prosthesis *Nat. Commun.* **9** 992